Experimental (FT-IR, FT-RS) and theoretical (DFT) studies of vibrational dynamics and molecular structure of 4- n-pentylphenyl-4′-n-heptyloxythiobenzoate (7OS5)

ARTICLE *in* JOURNAL OF MOLECULAR STRUCTURE · SEPTEMBER 2009

Impact Factor: 1.6 · DOI: 10.1016/j.molstruc.2009.05.051

3 AUTHORS, INCLUDING:

Diana Maria Dołęga
Jagiellonian University
6 PUBLICATIONS **23** CITATIONS

SEE PROFILE

Journal of Molecular Structure 933 (2009) 30–37

Contents lists available at ScienceDirect

Journal of Molecular Structure

journal homepage: www.elsevier.com/locate/molstruc

Experimental (FT-IR, FT-RS) and theoretical (DFT) studies of vibrational dynamics and molecular structure of 4-*n*-pentylphenyl-4′-*n*-heptyloxythiobenzoate (7OS5)

Diana Dołęga [a,*], Anna Migdał-Mikuli [a], Janusz Chruściel [b]

[a] Faculty of Chemistry, Jagiellonian University, Ingardena 3, 30-060 Kraków, Poland
[b] Faculty of Sciences, University of Podlasie, 3-go Maja 54, 08-110 Siedlce, Poland

ARTICLE INFO

Article history:
Received 6 April 2009
Accepted 28 May 2009
Available online 6 June 2009

Keywords:
Liquid crystal
Vibrational spectroscopy
Quantum chemical calculation
DFT calculation
Potential energy distribution
Hartree–Fock

ABSTRACT

Vibrational spectra of 4-*n*-pentylphenyl-4′-*n*-heptyloxythiobenzoate (7OS5) in the solid phase have been measured using Fourier transform infrared (FT-IR) and Raman scattering (FT-RS). Quantum chemical calculations using density functional theory (DFT) with functionals SVWN, B3PW91, MPW1PW91, PBEPBE, and B3LYP at the 6-31+G* basis set level were performed. Calculations using Hartree–Fock (HF) method with the same basis set were also carried out. Finally the complete assignments of the vibrational modes bands were performed on the basis of B3LYP/6-311+G** calculations. Ultimate geometry of molecule was also fixed. The assignments of the bands was based on the potential energy distribution (PED) data using the GAR2PED program. The general agreement between the observed and calculated frequencies are shown.

1. Introduction

In the present work, we have investigated 4-*n*-pentylphenyl-4′-*n*-heptyloxythiobenzoate, with formula: $H_{15}C_7O–C_6H_4–COS–C_6H_4–C_5H_{11}$, using later the acronym 7OS5, by infrared and Raman spectroscopy and by comparison of the experimental spectra with theoretical ones. The mesomorphic behaviour of this compound is characterized by the following enantiotropic phases and phase transitions:

$$\text{Crystal} \xrightarrow{331\ \text{K}} \text{Nematic} \xrightarrow{353\ \text{K}} \text{Isotropic liquid}.$$

The title compound belongs to the group of thermotropic liquid crystals in homologous series of the 4-*n*-pentylphenyl-4′-*n*-alkyloxythiobenzoates (*m*OS5), where *m* means a number of the carbon atoms in alkoxy-chain [1]. Despite their similar molecular structure the crystals which form this series exhibit very different polymorphism [2]. We believe that theoretical and spectroscopic structural analyzes, combined with crystallographic studies, may help to explain the nature of this polymorphism phenomenon [3,4]. Observation of vibrational bands of the most important functional groups makes it possible to achieve information about change of position both a flexible group and a joining bridge. Calamitic (rod-shaped) molecules forming liquid crystals systems are usually quite big and contain many atoms. Therefore they have rather rich vibrational spectra. By comparing of experimental spectra with the results of theoretical calculations we can obtain more complete and reliable structural information about their molecular system [1,3]. The theoretical methods based on density functional theory (DFT) are very important tool and widely used for the computation of molecular structure and vibrational frequencies especially for polyatomic systems [4–7].

2. Experimental

The 7OS5 sample was synthesized in the Institute of Chemistry of the University of Podlasie at Siedlce (Poland) by Ossowska-Chruściel [1]. The experimental infrared spectrum in the range of 400–50 cm^{-1} was recorded using a Fourier transform spectrometer Nicolet Magna-IR 760, equipped with a deuterium triglycine sulphate (DTGS) detector and with a Globar lamp as the light source. The spectrum was obtained with a spectral resolution of 1 cm^{-1}. Sample was in the solid state at room temperature. We have also collected spectrum in the range 4000–400 cm^{-1}. In this case it was used Fourier transform spectrometer Brucker EQUINOX 55 FT-MIR equipped with a highly sensitive mercury cadmium telluride (MCT) detector and a Nernst lamp as the light source. The spectrum was obtained with a spectral resolution of 4 cm^{-1}. Sample was in the solid state. Polarized light scattering spectrum was recorded using Fourier transform Raman scattering (FT-RS)

* Corresponding author. Tel.: +48 12 6632265; fax: +48 12 6340515.
E-mail address: diana.dolega@uj.edu.pl (D. Dołęga).

0022-2860/$ - see front matter © 2009 Elsevier B.V. All rights reserved.
doi:10.1016/j.molstruc.2009.05.051

spectrometer Thermo-Nicolet NXR 9650, equipped with germanium detector and using Nd–YAG laser, emitting light at 1064 nm. The FT-RS spectrum was collected in the range of 4000–100 cm^{-1}. One hundred fifty scans were performed with a spectral resolution of 4 cm^{-1} with a laser power of 471 mW for the polycrystalline sample.

3. Calculations

3.1. Molecular structure

In order to give detailed assignment of the vibrational spectra and consequently to solve the molecular structure we applied quantum mechanical calculations in frame of DFT and HF methods. All the calculations were performed using the Gaussian 03 [8] application running on a Baribal supercomputer at the Academic Computer Centre "Cyfronet" in Kraków. All the quantum chemical calculations were carried out with the GaussView molecular visualisation program [9]. A complete optimization of geometry was carried out employing following procedure. At first we had used optimized structure of shorter homologous compound 4OS5 using the molecular mechanics MM+ algorithm [1,10]. In the next step we carried out calculations by Austin model 1 (AM1), semi-empirical method for the obtained structure [10]. The total geometry optimization at the DFT level (SVWN, MPW1PW91, B3PW91, PBEPBE and B3LYP functionals) with basis set 6-31+G* were performed and vibrational frequencies were computed. *Ab initio* Hartree–Fock (HF) calculations at the same basis set were also done. The molecular geometry was optimized using the Becke three-parameter, Lee, Yang Parr hybrid functional (B3LYP) [7] with the basis set 6-311+G**. Next the optimized structure of 7OS5 was used to compute vibrational frequencies. All the optimized structures showed positive harmonic vibrations only (all eigenvalues are positive, no imaginary frequency indicates a true energy minimum [7,8]). As far as we know, there are no experimental data for the geometrical structure of 7OS5 molecule. Therefore we can not compare the theoretical geometric parameters with experimental values. Rauhut and Pulay [11] show, based on experimental data of 20 organic molecules, that B3LYP functional leads to geometry parameters close to experimental values. We base on these investigations and expect that B3LYP calculated geometry lead us to the most reliable molecular structure. The certain values of calculated bond lengths and angles for 7OS5 are included in Table 1. The atom numbering of 7OS5 and the molecular structure of investigated molecule 7OS5 is presented in Fig. 1, using program [9]. Main difference is observed in the φ dihedral angle between atoms: C_{19}–C_{18}–S_{17}–C_{15} which defines orientation of both phenyl rings. Phenyl rings are revealed in perpendicular orientation. Moreover, all the calculations predict that geometry in equilibrium state is linear. Additionally, PES (Potential Energy Surface) scan, which has been prepared by AM1 for 8SO5 homologous compound by Drużbicki et al. [8,12] revealed perpendicular geometry of the central group of atoms. We can conclude general agreement with data for homologous compounds presented in literature [1,12].

3.2. Molecular vibrations

We performed potential energy distribution (PED) calculations to show a detailed description of vibrational modes. For this reason we used GAR2PED program [13]. It is worth to mention that Gaussian 03 package calculate only Raman activities. To compare experimental and theoretical spectra Raman intensities are required. Therefore Raman intensities were determined from the RAINT [14] program using values of Raman scattering activities obtained from the Gaussian 03 outputs. Obtained vibrational frequencies are reported in Table 2. We employ calibrating procedure. This process is necessary for the HF method to correct for overestimation of vibrational frequencies due to vibrational anharmonicity and

Table 1
Selected angles values for equilibrium geometries obtained at the different levels of theory.

Method	$\theta_{C(15)-S(17)-C(18)}$	$\varphi_{C(10)-C(9)-O(8)-C(7)}$	$\varphi_{C(16)-C(15)-S(12)-C(13)}$	$\varphi_{C(19)-C(18)-S(17)-C(15)}$	$\varphi_{C(25)-C(24)-C(21)-C(20)}$
B3LYP 6-311+G(d,p)	100.76	0.35	−179.55	87.24	87.96
B3LYP 6-31+G(d)	100.97	0.08	−178.07	86.38	89.62
PBEPBE 6-31+G(d)	100.90	−0.08	−176.82	69.21	91.89
B3PW91 6-31+G(d)	100.82	0.50	−179.86	87.14	88.13
MPW1PW91 6-31+G(d)	100.63	0.45	−177.54	84.82	90.41
SVWN 6-31+G(d)	100.81	0.02	177.90	54.64	88.67
HF 6-31+G(d)	101.88	0.00	−179.89	91.22	89.31

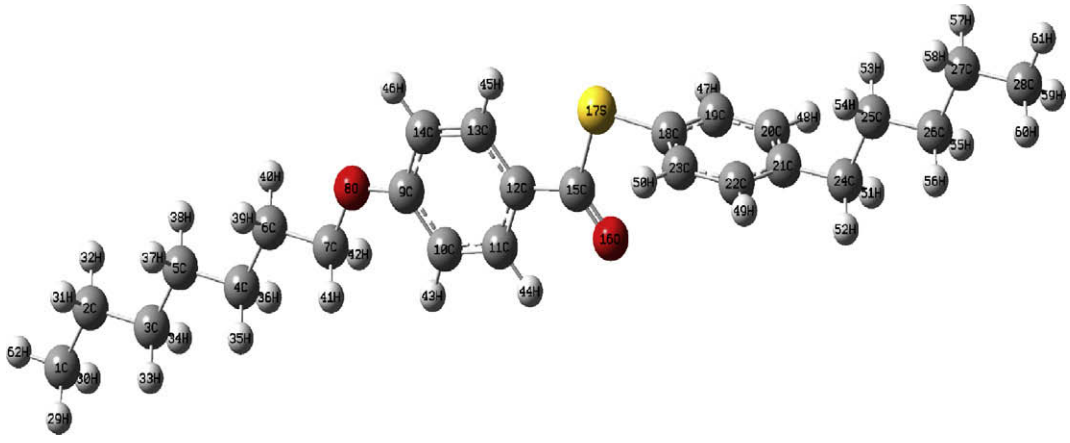

Fig. 1. A view of 7OS5 molecule with the atomic labelling.

Table 2
Vibrational frequencies, infrared and Raman intensities and their assignments.

No.	Experimental frequency		Calculated frequency		Intensities	Assignment (PED(⩾10%))
	IR	RS	Unscaled	Scaled	(IR, RS)*	
1.	–	–	10	10	(0.02,29.28)	$\tau C_{15}S_{16}(23) + \tau C_7O_8(14) + \tau C_{12}C_{15}(12)$
2.	–	–	14	14	(0.02,7.42)	$\tau S_{17}C_{18}(23) + \tau\ C_7O_8(12)$
3.	–	–	17	17	(0.01,8.72)	$\tau C_{12}C_{15}(32) + \tau C_{15}S_{17}\ (18)$
4.	–	–	22	22	(0.01,100)	$\tau S_{\ 17}C_{18}(53) - \tau C_{21}C_{24}(29)$
5.	–	–	28	28	(0.03,5.50)	$\rho C_4C_6C_7(15) + \tau C_{21}C_{24}(12) - \delta C_6C_7O_8(10)$
6.	–	–	33	33	(0.16,1.13)	$\tau C_{12}C_{15}(36) - \tau S_{17}C_{18}(19)$
7.	–	–	36	36	(0.01,16.51)	$\tau C_{21}C_{24}(34) - \tau S_{17}C_{18}(31)$
8.	–	–	42	42	(0.00,2.17)	$\tau C_6C_7(23) + \tau C_4C_5(17) + \tau C_4C_6(15)$
9.	–	–	49	49	(0.01,1.96)	$\tau C_{21}C_{24}(37) + \tau C_{24}C_{25}(26) + \tau C_{26}C_{27}(26)$
10.	55w	–	55	55	(0.05,12.08)	$\delta C_{15}S_{17}C_{18}(19) + \delta C_{21}C_{25}C_{24}(19) - \rho C_{22}C_{24}C_{21}(11)$
11.	69vw	–	58	58	(0.02,8.25)	$\tau O_8C_9(23) - \tau C_7O_8(17) - \tau C_{12}C_{15}(11) + \tau C_4C_6(11)$
12.	75vw	–	88	88	(0.15,3.66)	$\delta C_{11}C_{15}C_{12}(15) + \delta C_3C_4C_5(15) + \delta C_{12}S_{17}O_{16}C_{15}(11)$
13	95vw	–	95	95	(0.04,0.03)	$\tau C_2C_3(27) - \tau C_6C_7(23) + \tau C_9C_{10}C_{11}C_{12}C_{13}C_{14}(15)$
14.	102w	–	104	104	(0.02,0.30)	$\tau C_{25}C_{26}(38) - \tau C_3C_5(16)$
15.	–	–	106	106	(0.02,0.28)	$\tau C_{25}C_{26}(33) + \tau C_3C_5(17) - \tau O_8C_9(15)$
16	111w	111s	111	111	(0.07,4.08)	$\delta C_9O_8C_7(15) + \rho C_2C_5C_3(12)$
17.	145w	–	134	134	(0.22,0.14)	$\tau C_{26}C_{27}(24) + \tau O_8C_9(14)$
18.	148 m	–	135	135	(0.21,0.47)	$\tau C_{26}C_{27}(24) - \tau O_8C_9(14)$
19.	–	–	136	136	(0.06,0.81)	$\tau C_{25}C_{26}C_{27}(16) + \tau O_8C_9(14) + \rho C_{28}H3(13)$
20.	157 m	–	142	142	(0.10,0.14)	$\tau C_4C_6(40) - \tau C_3C_5(22) - \tau O_8C_9(15) + \tau C_{12}C_{15}(12)$
21.	163w	169 m	159	159	(0.20,0.32)	$\tau C_4C_5(33) - \tau C_6C_7(19) - \tau C_2C_3(18)$
22.	180w	182w	172	172	(0.15,2.55)	$\delta C_9O_8C_7(13) + \delta C_1C_3C_2(10)$
23.	213w	213vw	210	210	(1.23,0.31)	$\gamma^2C_{18}C_{19}C_{20}C_{21}C_{22}C_{23}(16) + \delta C_9O_8C_7(13) + \delta C_{15}S_{17}C_{18}(10)$
24.	–	–	237	237	(0.00,0.47)	$\delta C_4C_7C_6(16) + \delta C_1C_3C_2(16)$
25.	232vw	–	238	238	(0.00,0.02)	$\tau C_{27}C_{28}(89)$
26.	–	–	248	248	(0.00,0.01)	$\tau C_1C_2(92)$
27.	256vw	–	251	251	(0.04,0.09)	$\delta S_{17}C_{18}C_{23}(56) + \delta C_{21}C_{22}C_{24}(14)$
28.	269 m	269w	267	267	(9.53,3.91)	$\delta C_{12}C_{13}C_{15}(14) + \delta C_1C_3C_2(10)$
29.	287vw	–	293	293	(0.07,1.49)	$\gamma^2C_9C_{10}C_{11}C_{12}C_{13}C_{14}(36) + \tau C_{12}C_{15}(29)$
30.	303 m	303w	303	303	(5.50,2.30)	$\delta C_{25}C_{26}C_{27}(12)$
31.	367 m	–	358	358	(0.52,0.86)	$\delta C_{26}C_{27}C_{28}(42) + \delta C_{12}C_{15}S_{17}(14)$
32.			362	362	(0.35,0.67)	$\delta C_1C_2C_3(22) + \delta C_{24}C_{25}C_{26}(11)$
33.	377w	–	375	375	(0.02,0.29)	$\delta C_{22}C_{21}C_{24}(42) - \delta C_{15}S_{17}C_{18}(18)$
34	403w	–	376	376	(0.07,0.98)	$\delta C_{22}C_{21}C_{24}(11) - \delta C_3C_4C_5(10)$
35.	412	412w	417	417	(0.00,0.02)	$\gamma^3C_{18}C_{19}C_{20}C_{21}C_{22}C_{23}(83)$
36.			421	421	(0.08,2.67)	$\delta C_{25}C_{26}C_{27}(14) + \beta^2C_{18}C_{19}C_{20}C_{21}C_{22}C_{23}(11)$
37.	427w	427w	422	422	(0.00,0.13)	$\gamma^1C_9C_{10}C_{11}C_{12}C_{13}C_{14}(80)$
38.	443w	441w	435	435	(1.05,5.16)	$\delta^2\ C_{12}C_{15}{=}O_{16}S_{17}(27) - \rho S_{17}O_{16}C_{15}(14) + \gamma^2C_{18}C_{19}C_{20}C_{21}C_{22}C_{23}(10)$
39.	473w	–	458	458	(1.01,0.07)	$\gamma^2C_{18}C_{19}C_{20}C_{21}C_{22}C_{23}(15)$
40.	485 m	–	474	474	(0.08,0.88)	$\delta C_3C_5C_4(18) + \delta C_4C_6C_7(14) + \delta C_1C_2C_3(13) + \delta C_5C_6C_4(12)$
41.	499vw	506vw	508	508	(1.36,0.39)	$\gamma^2C_9C_{10}C_{11}C_{12}C_{13}C_{14}(32) + \omega C_7O_8C_9(31) - \gamma C_{15}C_{11}C_{13}C_{12}(15) + \gamma^2C_9C_{10}C_{11}C_{12}C_{13}C_{14}(10)$
42.	506w	517w	517	517	(2.20,5.61)	$\delta C_7O_8C_9(16) + \delta C_4C_6C_7(12) + \delta C_{10}C_9O_8(10)$
43.	527 m	527vw	546	546	(2.03,0.15)	$\gamma^3C_{18}C_{19}C_{20}C_{21}C_{22}C_{23}(29) + \gamma^2C_{18}C_{19}C_{20}C_{21}C_{22}C_{23}(16) - \gamma C_{15}S_{17}C_{18}(14)$
44.	568w	568w	574	574	(0.96,0.74)	$\beta^1C_9C_{10}C_{11}C_{12}C_{13}C_{14}(14) + \delta O_{16}C_{15}S_{17}(13) + \delta C_{15}S_{17}C_{18}(10) + \gamma^2C_{18}C_{19}C_{20}C_{21}C_{22}C_{23}(10)$
45.	625 m	631 m	642	629	(11.35,15.12)	$\beta^2C_9C_{10}C_{11}C_{12}C_{13}C_{14}(58)$
46.	–	–	646	633	(3.12,0.33)	$\gamma S_{17}C_{15}O_{16}(50) + \gamma^1C_9C_{10}C_{11}C_{12}C_{13}C_{14}(20) + \omega C\ H_{Ph1}(12)$
47.	–	–	651	638	(0.01,3.29)	$\beta^2C_{18}C_{19}C_{20}C_{21}C_{22}C_{23}(85)$
48.	660 m	660 m	662	649	(16.28,22.60)	$\beta^2C_9C_{10}C_{11}C_{12}C_{13}C_{14}(21) + \beta^3C_9C_{10}C_{11}C_{12}C_{13}C_{14}(20) + \nu C_{15}S_{17}(11)$
49.	–	–	674	661	(0.59,0.70)	$\nu S_{17}C_{18}(26) + \beta^1C_{18}C_{19}C_{20}C_{21}C_{22}C_{23}(25)$
50.	–	–	733	718	(0.75,0.02)	$\rho C_3H2(29) + \rho C_5H2(26) + \rho C_2H2(15) + \rho C_4H2(10)$
51.	–	721w	734	719	(0.48,0.01)	$\rho C_{26}H2(33) + \rho C_{25}H2(24) + \rho C_{27}H2(19)$
52.	–	–	738	723	(0.34,1.07)	$\gamma^1C_9C_{10}C_{11}C_{12}C_{13}C_{14}(59) + \gamma O_8C_9(16) + \gamma C_{12}C_{15}(14)$
53.	–	–	746	731	(0.03,0.02)	$\rho C_4H2(29) + \rho C_3H2(21) + \rho C_6H2(16)$
54.	775vw	–	754	739	(1.52,0.64)	$\beta^2C_{18}C_{19}C_{20}C_{21}C_{22}C_{23}(69) - \gamma C_{21}C_{24}(11)$
55.	–	–	760	745	(0.04,0.05)	$\rho C_{27}H2(31) + \rho C_{26}H2(25) + \rho C_{25}H2(16)$
56.	–	–	784	768	(0.34,0.07)	$\rho C_6H2(27) + \rho C_5H2(17) + \rho C_2H2(17)$
57.	–	–	822	806	(1.11,5.16)	$\beta^2C_{18}C_{19}C_{20}C_{21}C_{22}C_{23}(15) + \nu C_{21}C_{24}(14)$
58.	–	–	822	806	(0.09,0.11)	$\gamma H_{43}C_9C_{11}C_{10}(43) + \gamma H_{46}C_9C_{14}C_{13}(21) + \gamma H_{45}C_{14}C_{12}C_{13}(15) + \gamma H_{44}C_{10}C_{12}C_{11}(15)$
59.	833s	831w	833	816	(5.80,32.36)	$\nu O_8C_9(16) + \beta^1C_9C_{10}C_{11}C_{12}C_{13}C_{14}(13) + \nu C_9C_{10}(13)$
60.	–	–	844	827	(0.61,0.10)	$\gamma H_{48}C_{19}C_{21}C_{20}(18) + \gamma H_{47}C_{18}C_{20}C_{19}(15) - \gamma H_{49}C_{21}C_{23}C_{22}(17) + \gamma H_{50}C_{22}C_{18}C_{23}(15)$
61.	–	–	846	829	(4.79,0.04)	$\gamma H_{46}C_9C_{13}C_{14}(21) + \gamma H_{45}C_{14}C_{12}C_{13}(13) - \gamma H_{43}C_9C_{11}C_{10}(10)$
62.	–	–	848	831	(8.32,1.18)	$\gamma H_{48}C_{19}C_{21}C_{20}(18) + \gamma H_{47}C_{18}C_{20}C_{19}(15) + \gamma H_{49}C_{21}C_{23}C_{22}(13) + \gamma H_{50}C_{22}C_{18}C_{23}(10)$
63.	–	–	851	834	(0.55,0.16)	$\rho C_{26}H2(18) + \rho C_{25}H2(17) + \rho C_{28}H2(12) - \gamma H_{49}C_{21}C_{23}C_{22}(11) - \gamma H_{50}C_{22}C_{18}C_{23}(10)$
64.	–	–	856	839	(3.93,0.04)	$\gamma H_{43}C_9C_{11}C_{10}(12) + \gamma H_{45}C_{12}C_{13}C_{14}(10)$
65.	–	–	899	881	(1.38,1.02)	$\nu C_2C_3(28) + C_1H3(25)$
66.	–	–	904	886	(2.54,2.67)	$\nu C_{26}C_{27}(25) + C_{28}H3(23) + \nu C_{27}C_{28}(15)$
67.	904vs	899 m	908	890	(63.23,11.94)	$\delta^2C_{12}C_{15}O_{16}S_{17}(29) + \nu C_{15}S_{17}(14) - \nu C_{11}C_{12}(11) - \nu C_{12}C_{15}(11)$
68.	–	–	939	920	(0.01,0.11)	$\rho C_7H2(16) + \rho C_5H2(15) + \rho C_1H3(12) + \rho C_2H2(12) + \rho C_4H2(11)$
69.	–	–	970	951	(0.04,0.95)	$\gamma H_{50}C_{22}C_{18}C_{23}(21) + \gamma H_{47}C_{18}C_{20}C_{19}(20) + \gamma^2C_{18}Cs_{19}C_{20}C_{21}C_{22}C_{23}(18) - \gamma H_{48}C_{19}C_{21}C_{20}(16) - \gamma H_{49}C_{21}C_{23}C_{22}(17)$
70.	–	–	970	951	(0.01,0.02)	$\gamma H_{45}C_{14}C_{12}C_{13}(34) - \gamma H_{46}C_9C_{14}C_{13}(22) - \gamma H_{44}C_{10}C_{12}C_{11}(16) + \gamma H_{43}C_9C_{11}C_{10}(16)$
71.	–	–	973	954	(0.07,0.11)	$\rho C_{26}H2(18) + \rho C_{24}H2\ (17) + \rho C_{27}H2(15) + \rho C_{28}H2(14) + \rho C_{25}H2(13)$

Table 2 (*continued*)

No.	Experimental frequency		Calculated frequency		Intensities	Assignment (PED(⩾10%))
	IR	RS	Unscaled	Scaled	(IR, RS)*	
72.	–	–	983	963	(0.03,0.02)	$\gamma H_{50}C_{22}C_{18}C_{23}(23) - \gamma H_{47}C_{18}C_{20}C_{19}(23) + \gamma H_{48}C_{19}C_{21}C_{20}(22) - \gamma H_{49}C_{21}C_{23}C_{22}(22)$
73.	–	–	986	966	(0.19,0.03)	$\gamma H_{44}C_{10}C_{12}C_{11}(50) - \gamma H_{43}C_{9}C_{11}C_{10}(16) + \gamma H_{45}C_{14}C_{12}C_{13}(13) - \gamma H_{46}C_{9}C_{14}C_{13}(11)$
74.	974vw	–	996	976	(6.02,0.31)	$\nu C_4C_5(22) + \nu C_3C_5(22) - \nu C_1C_2(19)$
75.	–	–	1007	987	(0.33,4.06)	$\nu C_{24}C_{25}(25) + \nu C_{28}C_{27}(18) + \nu C_{25}C_{26}(12)$
76.	990 m	–	1022	1002	(5.29,0.60)	$\beta^1C_9C_{10}C_{11}C_{12}C_{13}C_{14}(30) - \nu C_4C_6(14) + \nu C_7O_8(13)$
77.	–	1016vw	1025	1005	(1.91,4.44)	$\beta^1C_9C_{10}C_{11}C_{12}C_{13}C_{14}(13) - \nu C_7O_8(13)+\nu C_4C_6(11) + \nu C_9C_{14}(11)$
78.	–	–	1028	1007	(0.11,0.03)	$\rho C_5H2(19) + \rho C_3H2(16) + \rho C_2H2(14)$
79.	1014 m	–	1033	1012	(0.74,3.38)	$\nu C_{24}C_{25}(27) + \beta^3C_{18}C_{19}C_{20}C_{21}C_{22}C_{23}(25) - \nu C_{25}C_{26}(17) + \nu C_{27}C_{28}(16)$
80.	1014 m	–	1034	1013	(3.11,0.43)	$\beta^1C_{18}C_{19}C_{20}C_{21}C_{22}C_{23}(42) + \nu C_{24}C_{25}(14)$
81.	1035w	–	1049	1028	(15.11,2.03)	$\nu C_7O_8(45) + \nu C_4C_6(17) - \nu C_6C_7(10)$
82.	–	–	1054	1033	(1.27,0.25)	$\nu C_1C_2(33) - \nu C_4C_6(17) - \nu C_2C_3(14) + \nu C_4C_5(14)$
83.	–	1060w	1062	1041	(0.06,4.52)	$\nu C_{25}C_{26}(35) - \nu C_{26}C_{27}(34) + \nu C_{27}C_{28}(23)$
84.	–	–	1066	1045	(0.14,3.62)	$\nu C_3C_5(36) - \nu C_4C_5(24) - \nu C_2C_3(12) + \nu C_4C_6(12)$
85.	1077vw	–	1084	1062	(1.02,0.65)	$\nu C_6C_7(42) - \nu C_2C_3(14)$
86.	1096w	1094 m	1094	1072	(0.25,0.10)	$\rho C_{24}H2(25) + \beta^1C_{18}C_{19}C_{20}C_{21}C_{22}C_{23}(12)$
87.	–	–	1107	1085	(0.55,46.38)	$\nu S_{17}C_{18}(24) - \nu C_{18}C_{19}(21) - \nu C_{18}C_{23}(21)$
88.	1116 m	1112w	1126	1103	(2.71,5.13)	$\delta C_{27}C_{28}H2(21) + \nu C_{26}C_{27}(17)$
89.	–	–	1140	1117	(0.78,0.10)	$\beta C_{21}C_{23}H_{49}C_{22}(14) + \beta C_{19}C_{20}H_{48}C_{21}(14) + \nu C_{19}C_{20}(13) - \nu C_{22}C_{23}(12)$
90.	–	–	1141	1118	(1.43,1.32)	$\beta C_9C_{13}H_{46}C_{14}(13) + \beta C_{10}C_{11}H_{44}C_{12}(12)$
91.	–	1128w	1144	1121	(3.72,7.02)	$\beta C_1C_2H_{62}(29)$
92.	1169s	1167 m	1184	1160	(100.00,46,08)	$\delta C_{10}C_{11}C_{12}(17) + \delta C_{12}C_{13}C_{14}(16) - \delta C_9C_{13}C_{14}(14) + \nu C_{12}C_{15}(13)$
93.	–	–	1187	1163	(0.39,0.37)	$\delta C_6C_7O_8(29) + \delta C_2C_3C_5(17) + \delta C_5C_4C_6(13)$
94.	–	1184w	1205	1180	(0.33,3.22)	$\beta C_{21}C_{23}H_{49}C_{22}(20) - \beta C_{19}C_{20}H_{48}C_{21}(20) + \beta C_{18}C_{19}H_{47}C_{20}(19) - \beta C_{18}C_{22}H_{50}C_{23}(19)$
95.	–	–	1223	1198	(0.13,0.22)	$\rho C_2H2(16) + \rho C_5H2(12) + \rho C_7H2(12) + \rho C_1H3(11)$
96.	–	–	1223	1198	(0.03,0.44)	$\rho C_{27}H2(20) - \rho C_{25}H2(15) + \rho C_{24}H2(14) + \rho C_{28}H3(13)$
97.	–	–	1224	1199	(2.95,5.84)	$\nu C_{21}C_{24}(37) + \beta^1C_{18}C_{19}C_{20}C_{21}C_{22}C_{23}(12)$
98.	1213s	1213 m	1229	1204	(35.70,55.3)	$\nu C_{12}C_{15}(36) + \beta C_9C_{10}H_{43}C_{11}(11) + \rho C_{10}H2(11) - \nu C_{10}C_{11}(10)$
99.	–	–	1253	1227	(0.08,0.11)	$\omega C_4H2(26) + \omega C_5H2(26) + \omega C_6H2(18) + \omega C_3H2(15)$
100.	–	1232 m	1265	1239	(0.01,0.78)	$\omega C_{25}H2(34) + \omega C_{26}H2(29) + \omega C_{24}H2(17)$
101.	–	1255	1271	1245	(0.07,0.28)	$\rho C_7H2(22) - \rho C_3H2(16) + \rho C_2H2(12) + \rho C_5H2(11)$
102.	1271s	1271vw	1285	1259	(0.09,0.67)	$\rho C_{27}H2(18) + \rho C_{24}H2(16) + \delta C_{21}C_{24}(14)$
103.	1271s	1271vw	1285	1259	(83.3,5.76)	$\nu O_8C_9(45)$
104.	–	–	1308	1281	(2.25,0.53)	$\omega C_6H2(29) - \omega C_3H2(27) - \omega C_2H2\ (16)$
105.	–	–	1313	1286	(0.01,0.14)	$\rho C_7H2(31) + \rho C_2H2(25) + \rho C_4H2\ (14)$
106.	–	–	1317	1290	(0.01,0.13)	$\nu C_{18}C_{23}(20) - \nu C_{18}C_{19}(20)$
107.	–	–	1325	1298	(0.01,6.42)	$\omega C_6H2(40) + \omega C_4H2(16) + \omega C_2H2(15) + \omega C_7H2(13) + \omega C_3H2(10)$
108.	–	1297 m	1327	1300	(0.02,0.70)	$\rho C_{25}H2(47)$
109.	–	–	1333	1306	(0.76,0.39)	$\beta C_{12}C_{13}H_{45}C_{14}(25) - \beta C_{10}C_{11}H_{44}C_{12}(21) - \beta C_9C_{10}H_{43}C_{12} + \beta C_9C_{13}H_{46}C_{14}(12)$
110.	–	–	1333	1306	(0.10,2.87)	$\omega C_{26}H2(48) + \omega C_{27}H2(32)$
111.	–	–	1336	1309	(0.17,4.44)	$\omega C_{24}H2(39) + \omega C_{25}H2\ (26) + \omega C_{27}H2(15)$
112.	–	–	1336	1309	(0.06,0.68)	$\omega C_3H2(38) + \omega C_5H2(31) + \omega C_6H2(16)$
113.	–	–	1340	1313	(0.05,0.05)	$\omega C_4H2(39) + \omega C_5H2(21) + \omega C_6H2(16)$
114.	1308s	1306 m	1342	1315	(25.24,9.67)	$\nu C_{11}C_{12}(22) - \nu C_{12}C_{13}(17) + \nu C_9C_{10}(17) - \nu C_9C_{14}(13)$
115.	–	–	1347	1320	(0.28,0.10)	$\rho C_{24}H2(19) - \beta C_{18}C_{22}H_{50}C_{23}(14) - \beta C_{18}C_{19}H_{47}C_{20}(14)$
116.	1324	–	1361	1333	(1.37,0.37)	$\omega C_2H2(29) + \omega C_5H2(22) + \omega C_6H2(17)$
117.	–	1350w	1379	1351	(0.08,6.34)	$\omega C_{25}H2(35) + \omega C_{27}H2(26) + \omega C_{24}H2(18)$
118.	–	–	1396	1368	(0.26,0.09)	$\omega C_2H2(27) + \omega C_7H2(23) + \omega C_4H2(21)$
119.	–	–	1398	1370	(0.19,0.08)	$\omega C_{26}H2(37) + \omega C_{25}H2(24) + \omega C_{27}H2(12) + \nu C_{26}C_{27}(10)$
120.	–	–	1403	1374,	(0.32,0.08)	$\omega C_5H2(28) + \omega C_3H2(19) + \omega C_4H2(16)$
121.	1377w	1376vw	1413	1384	(0.41,0.19)	$\omega C_{28}H3(89)$
122.	1377w	1376vw	1416	1387	(0.53,0.09)	$\omega C_1H3(85)$
123.	1402 m	1401w	1427	1398	(5.74,1.99)	$\nu C_7O_8(57) + \omega C_7H2(18) - \nu C_6C_7(10)$
124	1419w	–	1432	1403	(1.20,0.15)	$\nu C_{22}C_{23}(20) - \nu C_{19}C_{20}(20) + \beta C_{21}C_{22}H_{49}C_{23}(15) + \beta C_{19}C_{20}H_{48}C_{21}(15)$
125	–	–	1449	1420	(0.35,0.19)	$\nu C_{13}C_{14}(25) - \nu C_{10}C_{11}(25) + \beta C_9C_{13}H_{46}C_{14}(12) - \beta C_9C_{10}H_{43}C_{11}(11)$
126.	–	1437 m	1486	1456	(0.00,5.49)	$\delta C_{25}H2(57) + \delta C_{24}H2(20) + \delta C_{26}H2(14)$
127.	–	1437 m	1486	1456	(0.04,1.96)	$\delta C_3H2(55) + \delta C_2H2(19) + \delta C_5H2(10)$
128.	–	–	1487	1457	(0.02,1.27)	$\delta C_5H2(48) + \delta C_4H2(26) + \delta C_2H2(15)$
129.	–	–	1487	1457	(0.06,2.57)	$\delta C_{26}H2(44) + \delta C_{27}H2(41)$
130.	–	1447 m	1493	1463	(0.11,7.28)	$\delta C_4H2(32) + \delta C_2H2(27) + \delta C_6H2(24)$
131.	–	–	1495	1465	(0.36,3.10)	$\delta C_{28}H3(36) + \delta C_{24}H2(27) + \delta C_{27}H2(17) + \delta C_{26}H2(13)$
132.	–	–	1498	1468	(0.08,0.29)	$\delta C_6H2(35) + \delta C_1H3(25) + \delta C_3H2(16)$
133.	–	1468 m	1499	1469,	(1.59,1.46)	$\delta C_{28}H3(91)$
134.	–	–	1500	1470	(1.59,1.39)	$\delta C_1H3(91)$
135.	–	–	1505	1475	(0.01,0.12)	$\delta C_{28}H3(32) + \delta C_{24}H2(28) + \delta C_{25}H2(17) + \delta C_{27}H2(14)$
136.	–	–	1506	1476	(1.92,1.12)	$\delta C_1H3(26) + \delta C_7H2(17) + \delta C_4H2(16) + \delta C_5H2(12)$
137.	–	–	1513	1483	(2.03,0.07)	$\delta C_2H2(23) + \delta C_3H2(21) + \delta C_7H2(18) + \delta C_1H3(14) + \delta C_5H2(13)$
138.	–	–	1514	1484	(2.10,0.19)	$\delta C_{26}H2(25) + \delta C_{25}H2(24) + \delta C_{27}H2(21) + \delta C_{24}H2(12) + \delta C_{28}H3(11)$
139.	1494 m	1494vw	1519	1489	(9.88,0.17)	$\delta C_7H2(40) + \delta C_5H2(20) + \delta C_4H2(14)$
140.	–	–	1522	1491	(4.55,0.26)	$\beta C_{18}C_{19}H_{47}C_{20}(17) - \beta C_{18}C_{22}H_{50}C_{23}(17) + \beta C_{19}C_{20}H_{48}C_{21}(12) - \beta C_{21}C_{22}H_{49}C_{23}(12) - \nu C_{18}C_{19}(10) - \nu C_{18}C_{23}(10)$
141.	1509 m	1509w	1539	1508	(14.46,6.65)	$\beta C_{12}C_{13}H_{45}C_{14}(14) + \beta C_9C_{10}H_{43}C_{11}(13) + \beta C_{10}C_{11}H_{44}C_{12}(10)$
142.	–	1564vw	1602	1570	(0.01,0.47)	$\nu C_{20}C_{21}(19) - \nu C_{21}C_{22}(10) + \nu C_{18}C_{23}(17) + \nu C_{18}C_{19}(17) + \beta^2C_{18}C_{19}C_{20}C_{21}C_{22}C_{23}(10)$
143.	1565vw	–	1604	1572	(0.83,0.69)	$\nu C_9C_{10}(18) - \nu C_9C_{14}(17)+\nu C_{12}C_{13}(17) - \nu C_{17}C_{18}(16)$
144.	–	–	1635	1602	(3.19,22.38)	$\nu C_{19}C_{20}(21) + \nu C_{22}C_{23}(20)+\beta^2C_{18}C_{19}C_{20}C_{21}C_{22}C_{23}(10)$

(*continued on next page*)

Table 2 (*continued*)

No.	Experimental frequency		Calculated frequency		Intensities	Assignment (PED(⩾10%))
	IR	RS	Unscaled	Scaled	(IR, RS)*	
145.	1601vs	1597vs	1639	1606	(66.98, 100.00)	$\nu C_{13}C_{14}(23) + \nu C_{10}C_{11}(19) + \beta^2 C_9C_{10}C_{11}C_{12}C_{13}C_{14}(11)$
146.	1663vs	1662vs	1742	1707	(36.60,33.34)	$\nu C_{15}O_{16}(83)$
147.	–	–	2993	2873	(0.57,34.29)	$\nu C_3H_{33}(35) + \nu C_3H_{34}(34) - \nu C_4H_{36}(10)$
148.	–	–	2994	2874	(1.73,64.59)	$\nu C_{26}H_{56}(45) + \nu C_{26}H_{55}(45)$
149.	–	–	2995	2875	(0.61,25.58)	$\nu C_7H_{41}(16) + \nu C_7H_{42}(16) - \nu C_5H_{38}(14) - \nu C_4H_{36}(14) - \nu C_4H_{35}(13) - \nu C_5H_{37}(13)$
150.	–	2858 m	2998	2878	(1.44,86.87)	$\nu C_7H_{41}(28) + \nu C_7H_{42}(27) + \nu C_5H_{37}(15) + \nu C_5H_{38}(15)$
151.	–	–	3003	2883	(2.49,76.25)	$\nu C_4H_{36}(18) + \nu C_4H_{35}(18) + \nu C_2H_{32}(17) + \nu C_2H_{31}(17)$
152.	–	–	3005	2885	(1.07,1.43)	$\nu C_{27}H_{58}(27) + \nu C_{27}H_{57}(26) - \nu C_{25}H_{54}(22) - \nu C_{25}H_{53}(20)$
153.	2855s	–	3010	2890	(17.25,18.16)	$\nu C_2H_{32}(28) + \nu C_2H_{31}(26) + \nu C_5H_{38}(12)$
154.	–	–	3011	2891	(0.13,89.31)	$\nu C_3H_{33}(24) - \nu C_3H_{34}(23) - \nu C_5H_{37}(17) + \nu C_5H_{38}(14)$
155.	–	–	3012	2892	(5.13,100.00)	$\nu C_{25}H_{54}(20) + \nu C_{27}H_{58}(19) + \nu C_{25}H_{53}(18) + \nu C_{27}H_{57}(18)$
156.	–	–	3014	2893	(0.25,68.71)	$\nu C_{26}H_{55}(33) - \nu C_{26}H_{56}(33) - \nu C_{27}H_{59}(11) + \nu C_{27}H_{58}(11)$
157.	2869s	–	3018	2897	(0.74,75.41)	$\nu C_{28}H_{60}(36) + \nu C_{28}H_{59}(35) + \nu C_{28}H_{61}(25)$
158.	–	2884s	3018	2898	(9.03,6.51)	$\nu C_4H_{36}(23) - \nu C_4H_{35}(23) - \nu C_2H_{31}(10)$
159.	–	–	3019	2898	(9.03,84.20)	$\nu C_1H_{30}(35) + \nu C_1H_{29}(32) + \nu C_1H_{62}(24)$
160.	–	2911s	3023	2902	(69.95,41.22)	$\nu C_{24}H_{51}(40) + \nu C_{24}H_{52}(37)$
161.	–	–	3029	2908	(8.85,30.57)	$\nu C_6H_{40}(50) + \nu C_6H_{39}(44)$
162.	–	–	3032	2911	(0.46,0.21)	$\nu C_{25}H_{53}(22) - \nu C_{29}H_{57}(21) + \nu C_{27}H_{58}(21) - \nu C_{25}H_{54}(24)$
163.	–	–	3033	2911	(1.55,44.05)	$\nu C_7H_{41}(20) - \nu C_4C_6(20) - \nu C_2H_{31}(11) + \nu C_2H_{32}(10) - \nu C_6H_{39}(10)$
164.	–	–	3035	2914	(1.56,1.01)	$\nu C_7H_{42}(20) - \nu C_7C_{42}(66) + \nu C_2H_{32}(12) - \nu C_2H_{31}(12)$
165.	–	–	3045	2923	(2.67,29.29)	$\nu C_{24}H_{52}(16) - \nu C_{24}H_{51}(14) + \nu C_{27}H_{57}(12) + \nu C_{27}H_{58}(12) + \nu C_{26}H_{56}(12) + \nu C_{26}H_{55}(12)$
166.	2926s	2926s	3050	2928	(10.63,3.03)	$\nu C_5H_{37}(18) - \nu C_5H_{38}(18) - \nu C_3H_{34}(14) + \nu C_3H_{33}(14)$
167.	–	–	3065	2943	(9.00,2.42)	$\nu C_{24}H_{52}(30) - \nu C_{24}H_{51}(29) - \nu C_{25}H_{53}(16) + \nu C_{25}H_{54}(15)$
168.	–	–	3074	2951	(12.21,6.58)	$\nu C_6H_{39}(39) - \nu C_6H_{40}(37)$
169.	–	–	3079	2955	(14.61,16.70)	$\nu C_{28}H_{60}(44) - \nu C_{28}H_{59}(42)$
170.	–	–	3079	2955	(16.71,13.56)	$\nu C_1H_{29}(44) - \nu C_1H_{30}(43)$
171.	–	2960s	3082	2959	(8.86,58.21)	$\nu C_{28}H_{61}(73) - \nu C_{28}H_{59}(14) - \nu C_{28}H_{60}(12)$
172.	2957s	–	3084	2961	(8.93,55.56)	$\nu C_1H_{62}(74) - \nu C_1H_{30}(14) - \nu C_1H_{29}(11)$
173.	3038w	3038s	3157	3031	(2.44,41.05)	$\nu C_{22}H_{49}(67) - \nu C_{20}H_{48}(27)$
174.	–	–	3158	3032	(3.70,40.42)	$\nu C_{20}H_{48}(66) + \nu C_{22}H_{49}(26)$
175.	–	–	3185	3058	(1.70,15.78)	$\nu C_{13}H_{45}(64) - \nu C_{14}H_{46}(34)$
176.	3058w	–	3189	3062	(1.91,4.14)	$\nu C_{23}H_{50}(52) - \nu C_{19}H_{47}(42)$
177.	3060vw	3060w	3191	3063	(0.01,70.50)	$\nu C_{19}H_{47}(51) + \nu C_{23}H_{50}(40)$
178.	–	–	3194	3066	(0.04,16.03)	$\nu C_{11}H_{44}(77) - \nu C_{10}H_{43}(21)$
179.	–	–	3200	3072	(0.39,54.05)	$\nu C_{14}H_{46}(65) + \nu C_{13}H_{45}(34)$
180.	–	–	3210	3082	(2.63,59.38)	$\nu C_{10}H_{43}(78) + \nu C_{11}H_{44}(21)$

ν – Stretching mode, ρ – rocking mode, ω – wagging mode, δ – scissoring mode, β – in-plane-deform, γ – out-of-plane-deform, τ – torsion mode, β^1 – trigonal deformation, β^2 – anti-symmetric deformation the first type, β^3 – anti-symmetric deformation the second type, γ^1 – puckering mode, γ^2 – anti-symmetric torsion the first type, γ^3 – anti-symmetric torsion the second type, low index – labeled atom, vw – very weak, w – weak, sh – shoulder, m – medium, s – strong, vs – very strong.

* Percentage relative intensity with respect to the most intensive bands. For FT-IR unscaled calculated spectrum the most intensive band is 1184 cm^{-1}, in FT-RS unscaled spectrum there are bands at 22, 1639 and 3012 cm^{-1}.

neglecting electron correlation the case of DFT methods calibrating factors are used to compensate incomplete incorporation of electron correlation, as well as to account of vibrational anharmonicity [11,15–17]. We did not calibrated the range between 400 and 50 cm^{-1}. In the wave number range 2000–400 cm^{-1} obtained frequencies were multiplied by factor 0.98. The frequencies from the last area 3500–2000 cm^{-1} were multiplied by ratio 0.96. This is consistent with the recommendation Pople et al. [16,17] The obtained experimental spectra (FT-IR, FT-RS) are compared with fitted calculated spectra by five different functionals and 6-31+G*

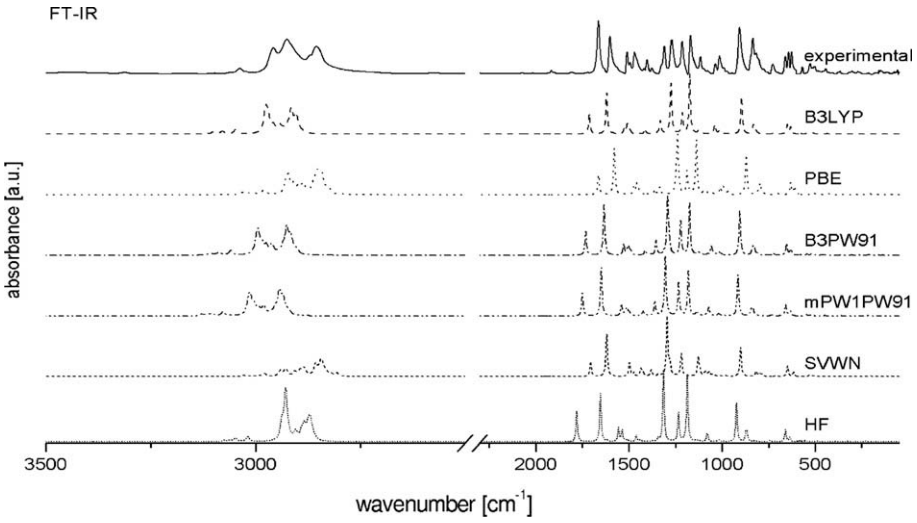

Fig. 2. The comparison of both experimental and scaled theoretical FT-IR spectra for 7OS5 in the region between wavenumbers 2260–50 and 3500–2500 cm^{-1} (different functionals/6-31+G*).

basis set are presented in Figs. 2 and 3. Calculated RMS (Root Mean Square) show that hybrid B3LYP functional gives quite good reproduction of experimental frequencies. Intensities relations achieved in the calculations with B3LYP correspond to experimental values pretty well. The experimental and theoretical, calculated with B3LYP functional and higher 6-311+G** basis set, vibrational spectra were shown in Figs. 4 and 5, for FT-IR and FT-RS, respectively. Figs. 4a, b and 5a, b present calibrated ranges. Far-infrared area of the frequency spectrum is no scaled. Additionally, calculated Dirac delta were shown as spectral lines. We have presented Lorentzian broadening of calculated peaks, which facilitates comparison of calculated spectrum with the experimental one. In the Table 2. We can see the scaled and unscaled values of frequencies calculated on the B3LYP/6-311+G** level of theory. We have

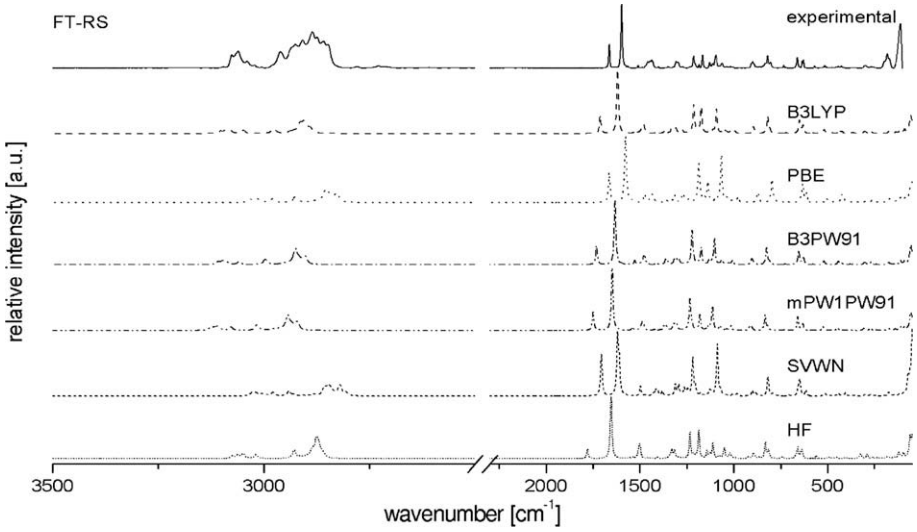

Fig. 3. The comparison of both experimental and scaled theoretical FT-RS spectra for 7OS5 in the region between wavenumbers 2260–50 and 3500–2500 cm^{-1} (different functionals/6-31+G*).

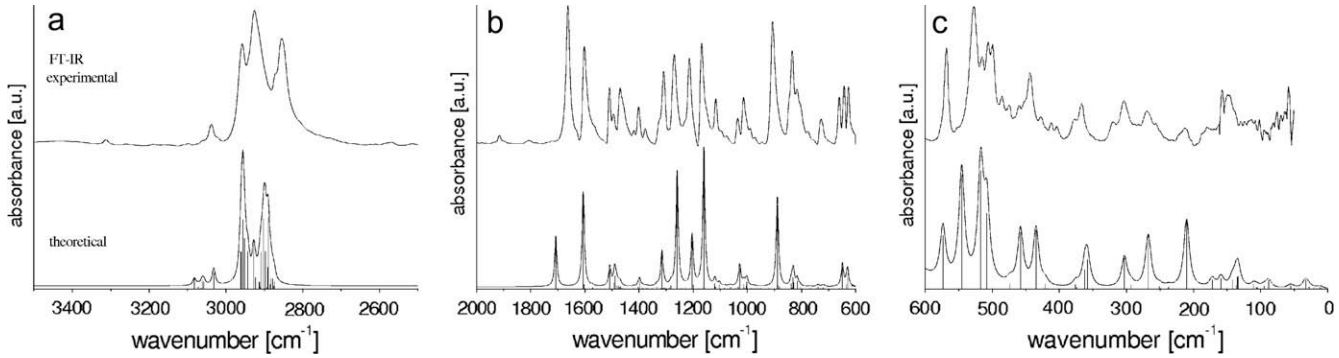

Fig. 4. The comparison of both experimental and theoretical FT-IR spectra for 7OS5 (B3LYP/6-311+G**). (a) The unscaled range 50–600 cm^{-1}, (b) the scaled range 600–2000 cm^{-1} (Scaling factor 0,98), and (c) the scaled range 2000–3500 cm^{-1} (Scaling factor 0,96).

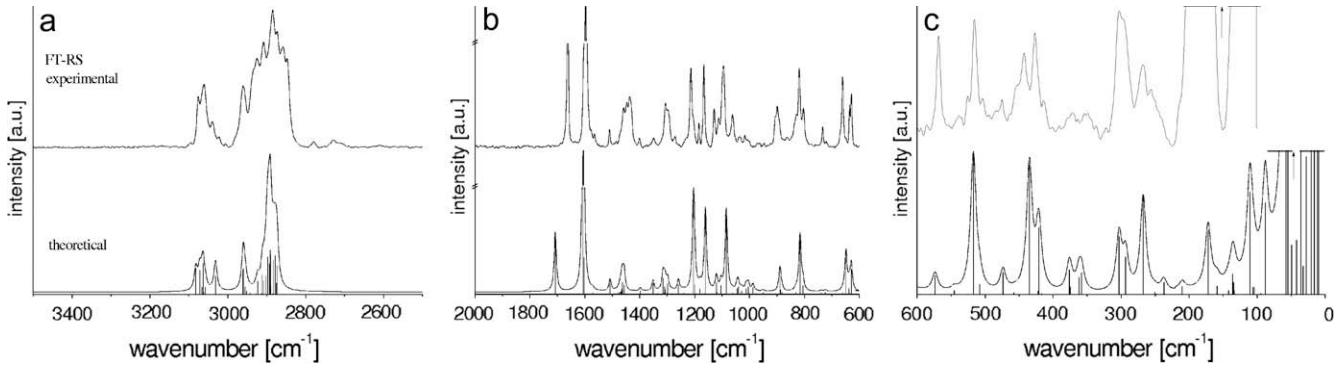

Fig. 5. The comparison of both experimental and theoretical FT-RS spectra for 7OS5 (B3LYP/6-311+G**). (a) The unscaled range 50–600 cm^{-1}, (b) the scaled range 600–2000 cm^{-1} (Scaling factor 0,98), and (c) the scaled range 2000–3500 cm^{-1} (Scaling factor 0,96).

normalized theoretical FT-IR spectrum to the most intensive frequency. The calculated FT-RS spectrum has been normalized in three ranges 3500–1800, 1800–600 and 600–50 cm^{-1}.

4. Results and discussion

According to the DFT and group theory results 7OS5 has 180 fundamental vibrations. The calculated frequencies of normal vibrations of 7OS5 from the B3LYP functional with 6-311+G** basis set have been compared with infrared and Raman results for compound in the solid state. All calculations were performed assuming C1 point group symmetry for 7OS5 molecule. It should be emphasized ones more that the simulated spectra refer to the isolated molecule at 293 K, whereas the assignments are made for the vibrational spectra of the solid state at room temperature. Thus, some differences in the calculated versus experimental frequencies or intensities are most probably caused by intermolecular interactions (crystal packing) and/or by anharmonicity of the vibrations, limited range of interactions between atoms and basis set. However, we can see that experimental and theoretical spectra are very similar. Hence, we conclude that intermolecular interactions in this solid state are very weak.

The computed frequencies, compared with the experimental data are given in Table 2. With our calculations we predict the torsion motions in the range 55–232 cm^{-1} especially in the alkylo- and alkoxy-chains. At 252 cm^{-1} deformative mode of –CSC-molecular group can be observed. As we can see in Figs. 2 and 3, fundamentals achieved from experimental far-infrared and Raman measures are relatively low intense. Comparison of both 7OS5 and 8OS5 compounds lead us to small differences in the far-infrared range, below 252 cm^{-1}. However, it can be observed there torsion motions of the chains [12]. Calculations at the 300–400 cm^{-1} region allow us to assign scissoring motions of these chains. The corresponding bands in 8OS5 in the range of skeletal groups are shifted of several cm^{-1} [12]. Moreover, the calculations predict out-of-plane motions at 417 and 427 cm^{-1} of the both phenyl rings, which correspond to weak peaks at 412 and 427 cm^{-1} of the experimental infrared and Raman spectra. The fundamental at 443 cm^{-1} (IR experimental spectrum) and 441 cm^{-1} (RS experimental spectrum) we assigned mainly to the bridge vibrations. The next bands, at 500 cm^{-1} (IR) and 506 cm^{-1} (RS), are found to be out-of-plane motions of phenyl ring associated with alkoxy-chain. Similar kind of vibrations of the second ring can be observed both in IR and RS experimental spectra. Bands in the range of 420–530 cm^{-1} of 7OS5 compared with these of 8OS5 compound have small differences between intensities relations [12]. Vibrations of the joining bridge and phenyl ring appear in the range of 568–660 cm^{-1} at the experimental spectra. The intensities and frequencies of bands of the 8OS5 compound are overlapped is with a maximal deviation of 3 cm^{-1} [12].

Our calculations predict that the medium intensity fundamentals at 660 cm^{-1} are found to deform-in-plane phenyl rings. Weak band at 721 cm^{-1} on Raman spectrum is especially caused by the rocking CH_2 motions in alkoxy-chain. The same band is observed for 8OS5 compound [12]. Very weak intense band in infrared spectrum at 775 cm^{-1} corresponds with of out-of-plane vibration of phenyl ring from our calculations. Signals in area 833 cm^{-1} (IR spectrum) and 831 cm^{-1} (RS spectrum) represent stretching motions of alkoxy-chain and associated phenyl ring. We have noticed that respective bands for 8OS5 are shifted and have different integral intensity [12]. One of the most intensive peaks in the infrared spectrum is related with rocking motion of joining bridge, namely thioester group (–COS–). We can also note stretching vibration of sulphur atom associated with carbon atom from phenyl ring. Frequencies from 974–990 cm^{-1} to 1035–1077 cm^{-1} ranges in the infrared spectrum represent stretching motions from heptyloxy terminal group. There are no significant quantitative differences at 8OS5 spectrum. However, band recorded at about 1016 and 1060 cm^{-1} has been assigned to the stretching vibrations of terminal group ($-C_5H_{11}$) of investigated molecular system [12]. Also this part of spectrum gives characteristic band because of motions in phenyl rings. Signals at 1096 and 1094 cm^{-1} in infrared and Raman spectra are assigned to the rocking motions of two atoms of hydrogen associated with carbon atom no. 24 (Fig. 1). However, Drużbicki et al. [12] show that this bands belong to the stretching motion of –C–S–. There is also small contribution of relevant phenyl ring. Predicate upon potential energy distribution calculations, small intensive peak on Raman spectrum, at frequency 1128 cm^{-1} represent skeletal modes of heptyloxy-chain and deform-in-plane motions of hydrogen atoms in associated phenyl ring. The most intensive band in infrared spectrum at 1169 cm^{-1} corresponding to that at 1167 cm^{-1} on Raman spectrum and is caused by deformation motions of carbon atoms with numbers: from 9 to 14 in the first phenyl ring. Weak intensive mode at frequency 1184 cm^{-1} in Raman experimental spectrum mainly has been assigned to the hydrogen in-plane motions of the second phenyl ring. Towards higher frequency both Raman and infrared experimental spectra are present peaks at frequency 1213 cm^{-1} strong and weak intensity, respectively, alike at [12]. Those bands are caused by stretching modes between the carbon atom in thioester group and associated carbon from phenyl ring, especially. There are also some contributions of vibrations in the phenyl ring. The band recorded at 1232 cm^{-1} on Raman spectrum corresponds to wagging motions of hydrogen atoms in terminal ($-C_5H_{11}$) alkylo-group. However, this band is absent in 8OS5 spectra [12]. While the following band on this spectrum give much contributions by rocking motions of hydrogen atoms in the second alkoxy-terminal group. Intensive band at 1271 cm^{-1} in the FT-IR spectrum and very weak band in the FT-RS spectrum comes from the stretching mode. The vibrations are connected with alkoxyphenyl group O_8–C_9 (45% PED). Rocking motions of CH_2 alkylo-group has been ascribed to the medium intensive band in Raman spectrum. While no significant differences are observed for the related bands in the homologous compound 8OS5 [12]. Stretching vibrations of phenyl ring correspond to strong band in the infrared spectrum at frequency 1308 and 1306 cm^{-1} in the FT-RS spectrum. Wagging CH_2 motions of heptyloxy-fragment appear at 1324 cm^{-1} in the infrared spectrum. The same kind of vibrations appears in the Raman spectrum at 1350 cm^{-1}. It is concerned with alkylo- ($-C_5H_{11}$) group. Motions of two methyl ($-CH_3$) groups in 7OS5 give rather big contributions to the bands in the region of 1377 cm^{-1} (both spectra). Further around 1402 cm^{-1} there is present peak, which comes from stretching vibrations of oxygen atom in hepyloxy- (C_7–O_8) tail. There are also some contributions of wagging motions (CH_2) and stretching motions between carbon atoms in this molecular fragment. Medium intensive signals in the FT-RS spectrum at region 1437–1468 cm^{-1} is assigned to deform scissoring motions of hydrogen atoms in alkylo-group. Calculations show that observed bands both infrared and Raman spectra at 1494 cm^{-1} comes from rocking modes in heptyloxy tail. Deform-in-plane vibrations of both phenyl rings cause emerging signals in the range 1509–1609 cm^{-1} in the vibrational spectra. Stretching bending of carbonyl group C_{15}=O_{16} can be observed as a very strong band in both spectra at 1662 cm^{-1}. With our calculations we predict respectively rich contribution (83% PED). The ν(C=O) peak for analogous 8OS5 which informs about similar interaction was recorded at 1665 cm^{-1} (in both spectra) [12]. The last region is connected with stretching vibrations between carbon atoms and hydrogen atoms both terminal fragments of 7OS5 in the investigated compound. Theoretical calculations also show stretching modes of CH groups in both phenyl rings. According to Drużbicki et al. [12] there were not observed significant differences in this spectral range.

5. Conclusions

The spectra of both 7OS5 and 8OS5 compounds are very similar (see Ref. [12]). The experimental vibrational spectra of 7OS5 molecule are rather rich. It is caused by overtones and combinational bands. Theoretical computations could not reproduce exactly experiment by using of selected model. Results of calculations show that B3LYP functional and relatively high 6-311+G** basis set is quiet good to be compared with experiment. In summary, a complete vibrational assignments of investigated compound is obtained from these studies in addition to supplying normal mode descriptions and PED values for the vibrational frequencies. We can also conclude, that good agreement between the experiment and theory, which was obtained despite the fact that the spectra were recorded in the crystalline state and the computations were based on the isolated molecule model, suggests existence of very weak interactions, probably dispersive, between the molecules of 4-*n*-pentylphenyl-4′-*n*-heptyloxythiobenzoate in the crystal lattice.

Acknowledgments

Calculations were done at the Academic Computer Centre "Cyfronet", Kraków, Poland which is acknowledged for computing time (Grant number: MNiSW/SGI3700/UJ/009/2009).

References

[1] M.D. Ossowska-Chruściel, Z. Karczmarzyk, J. Chruściel, Mol. Cryst. Liq. Cryst. 382 (2002) 37.
[2] J. Chruściel, PhD disseration, Jagiellonian University, Cracow, 1978.
[3] R. Korlacki, K. Merkel, J.K. Vij, R. Wrzalik, A. Kocot, M.D. Ossowska-Chruściel, J. Chruściel, S. Zalewski, Liq. Cryst. 33 (2006) 219.
[4] A. Kocot, G. Kruk, R. Wrzalik, J.K. Vij, Liq. Cryst. 12 (1992) 1005.
[5] D. Bauman, E. Mykowska, A. Zięba, E. Chrzumnicka, G. Czechowski, J. Jadżyn, Phase Trans. 80 (2007) 599.
[6] R. Wrzalik, K. Merkel, A. Kocot, B. Cieplak, J. Chem. Phys. 117 (2002) 10.
[7] J.B. Foresman, A.E. Frish, Exploring Chemistry with Electronic Structure Methods, Gaussian, Pittsburgh, 1998.
[8] M.J. Frisch, G.W. Trucks, H.B. Schlegel, G.E. Scuseria, M.A. Robb, J.R. Cheeseman, J.A. Montgomery Jr., T. Vreven, K.N. Kudin, J.C. Burant, J.M. Millam, S.S. Iyengar, J. Tomasi, V. Barone, B. Mennucci, M. Cossi, G. Scalmani, N. Rega, G.A. Petersson, H. Nakatsuji, M. Hada, M. Ehara, K. Toyota, R. Fukuda, J. Hasegawa, M. Ishida, T. Nakajima, Y. Honda, O. Kitao, H. Nakai, M. Klene, X. Li, J.E. Knox, H.P. Hratchian, J.B. Cross, V. Bakken, C. Adamo, J. Jaramillo, R. Gomperts, R.E. Stratmann, O. Yazyev, A.J. Austin, R. Cammi, C. Pomelli, J.W. Ochterski, P.Y. Ayala, K. Morokuma, G.A. Voth, P. Salvador, J.J. Dannenberg, V.G. Zakrzewski, S. Dapprich, A.D. Daniels, M.C. Strain, O. Farkas, D.K. Malick, A.D. Rabuck, K. Raghavachari, J.B. Foresman, J.V. Ortiz, Q. Cui, A.G. Baboul, S. Clifford, J. Cioslowski, B.B. Stefanov, G. Liu, A. Liashenko, P. Piskorz, I. Komaromi, R.L. Martin, D.J. Fox, T. Keith, M.A. Al-Laham, C.Y. Peng, A. Nanayakkara, M. Challacombe, P.M.W. Gill, B. Johnson, W. Chen, M.W. Wong, C. Gonzalez, J.A. Pople, Gaussian 03, Revision D.01, Gaussian, Inc., Wallingford, CT, 2004.
[9] W. Gaussview, Æ. Frish, A.B. Nielsen, A.J. Holder, Gaussian Inc., Carnegie Office Park, Building 6, Pittsburg, PA 15106, USA.
[10] A.R. Leach, Molecular Modelling. Priciples and Application, second ed., Pearson Education EMA, Prentice–Hall, 2001, p. 773.
[11] G. Rauhut, P. Pulay, J. Phys. Chem. 99 (1995) 3093.
[12] K. Drużbicki, E. Mikuli, M.D. Ossowska-Chruściel, Vib. Spectrosc. in press.
[13] J.M.L. Martin, C. Van Alsenoy, Gar2ped, University of Antwerp, 1995.
[14] R. Wysokiński, D. Michalska, Chem. Phys. Lett. 403 (2005) 211.
[15] M. Barańska, K. Chruszcz, B. Poduszek, L.M. Proniewicz, Vib. Spectrosc. 31 (2003) 291.
[16] J.A. Pople, A.P. Scott, M.W. Wong, L. Radom, Isr. J. Chem. 33 (1993) 345.
[17] J.A. Pople, H.B. Schlegel, R. Krishnan, D.J. Defrees, J.S. Binkley, M.J. Frisch, R.A. Whiteside, R.F. Hout, W.J. Hehre, Int. J. Quant. Chem. S15 (1981) 269.